Japan Bilingual Publishing Co.

Urban Planning and Construction

https://ojs.bilpub.com/index.php/upc

ARTICLE

From Flood Mapping to Planning-Relevant Flood Intelligence: A Sentinel-1 SAR-Based Framework for Urban Planning and Climate Adaptation in Valencia, Spain

Arezoo Salamatnia

Independent Researcher, Tehran 1476616539, Iran

ABSTRACT

Flooding is among the most destructive natural hazards affecting urban environments worldwide, with its frequency and severity increasingly worsened by climate change and rapid urban expansion. This study presents an operational flood detection framework based on multi-temporal Sentinel-1 Synthetic Aperture Radar (SAR) imagery, applied to the severe flooding event in Valencia, Spain, in late 2024. The proposed workflow integrates pre- and post-event SAR acquisitions within a systematic processing chain that includes radiometric calibration, speckle noise reduction, and multi-temporal change detection. Flood delineation was achieved through threshold-based segmentation and post-classification refinement and independently validated against the Copernicus Emergency Management Service (EMS) rapid-mapping product, achieving an overall agreement of approximately 87%. The analysis identified an inundation extent of 4.96 km^2, primarily in the western and northwestern sectors of Valencia. To enhance the practical relevance of the remote sensing results, this study develops a conceptual framework linking satellite-derived flood information with urban resilience planning and disaster risk management objectives. Rather than focusing solely on flood detection performance, the study emphasizes the translation of satellite-derived flood information into planning-relevant knowledge through measurable SDG-oriented planning indicators that support resilience-oriented urban governance. The framework demonstrates how spatial flood intelligence can support monitoring and decision-making processes related to Sustainable Development Goal (SDG) Targets 11.5, 11.b, and 13.1. By connecting satellite-based flood observations with policy-oriented urban planning

*CORRESPONDING AUTHOR:
Arezoo Salamatnia, Independent Researcher, Tehran 1476616539, Iran; Email: arezoosalamatnya@gmail.com

ARTICLE INFO
Received: 12 February 2026 | Revised: 16 May 2026 | Accepted: 23 May 2026 | Published Online: 30 May 2026
DOI: https://doi.org/10.55121/upc.v4i1.101402

CITATION
Salamatnia, A., 2026. From Flood Mapping to Planning-Relevant Flood Intelligence: A Sentinel-1 SAR-Based Framework for Urban Planning and Climate Adaptation in Valencia, Spain. Urban Planning and Construction. 4(1): 81–101. DOI: https://doi.org/10.55121/upc.v4i1.101402

frameworks, the proposed workflow provides evidence-based support for risk-sensitive land-use planning, infrastructure prioritization, evacuation planning, and post-disaster recovery while offering a transferable framework for municipal disaster risk management and urban resilience.

Keywords: Flood Intelligence; Sentinel-1 SAR; Urban Flood Mapping; Climate Adaptation; Conceptual Framework

1. Introduction

Climate change is increasing the frequency and severity of extreme hydrometeorological events, further challenging metropolitan regions worldwide. The authors strengthen the observational basis for this finding by documenting the rising frequency and severity of coastal and compound flood hazards at several monitoring stations [1]. Disaster risk management must now shift from reactive measures to proactive, data-driven strategies. Among the available technologies, multitemporal Sentinel-1 Synthetic Aperture Radar (SAR) imagery has become an essential tool for operational flood mapping, as it can penetrate cloud cover and operate under adverse weather conditions, enabling continuous data acquisition [2, 3].

This functionality was essential for the Valencia event, as the Depresión Aislada en Niveles Altos (DANA) storm system that caused the October 2024 flooding was characterized by thick, persistent cloud cover. This would have prevented timely optical observation of the affected areas, making radar-based monitoring the only way to obtain continuous imagery during the event.

Besides the direct environmental impacts, floods pose a major challenge for urban planning and infrastructure management. As cities expand into hazard-prone areas, integrating geospatial information into planning processes has become essential to strengthen urban resilience, reduce disaster risk, and support sustainable urban development [4–6].

Despite the growing availability of satellite-derived flood information, transforming geospatial flood products into practical planning knowledge to support urban resilience and climate adaptation strategies remains a significant challenge. To address this in a practical setting, this paper employs a case study design: it applies an operational Sentinel-1 SAR flood-mapping workflow to the October 2024 Valencia flood event and uses the resulting flood-extent product as the empirical basis for developing and illustrating a planning-oriented conceptual framework, rather than presenting a purely methods-focused comparison of detection techniques.

The effectiveness of SAR-based flood detection depends on advanced signal processing and the integration of auxiliary spatial data, since dense urban settlements and complex topography require flood-mapping algorithms robust to speckle noise and layover effects [3, 7].

Building on these insights, recent methodological advancements couple SAR-derived change statistics with hydrological and machine-learning models to improve detection accuracy, though threshold-based segmentation remains attractive for its transparency and low computational cost [8, 9].

At the international level, disaster risk reduction and climate adaptation have become central components of sustainable urban development. Empirical studies confirm that integrating satellite-derived geospatial information into municipal resilience planning measurably reduces disaster losses and improves adaptive capacity to climate-related hazards [10–12]. Consequently, there is a growing demand for operational geospatial information that can support evidence-based urban planning and resilience-oriented decision-making, an alignment we frame here with reference to SDG Targets 11.5, 11.b, and 13.1 [13].

This study proposes a practical operational workflow, combining multi-temporal SAR data with robust remote sensing techniques, that translates satellite-derived flood information into planning-relevant knowledge supporting both immediate flood response and long-term urban resilience, climate adaptation, and disaster risk management.

While policy frameworks such as the United Nations Office for Disaster Risk Reduction (UNDRR) (2022) and the Intergovernmental Panel on Climate Change (IPCC) (2022) articulate the conceptual need for this translation at the level of international guidance, they stop short of providing an empirical, case-level demonstration of how a specific satellite-derived flood product can be operationally and quantitatively linked to planning indicators; it is this empirical and operational gap, rather than a lack of conceptual recognition, that the present study addresses [5, 6]. Consequently, a gap remains between technical flood mapping outputs and their application within policy-oriented disaster risk reduction and climate adaptation strategies, a gap also noted in recent reviews of operational flood-information uptake [3]. The primary objective of this study is to develop a planning-oriented framework that demonstrates how satellite-derived flood information from multi-temporal Sentinel-1 SAR imagery can support urban planning, disaster risk management, and climate adaptation processes.

In addition to its technical focus, this research embeds the methodological workflow within a sustainability perspective aligned with SDG 11 (Sustainable Cities and Communities) and SDG 13 (Climate Action) [13].

More specifically, the study aims to: (i) develop a planning-oriented framework illustrating how satellite-derived flood information can support urban planning, disaster risk reduction, and climate adaptation processes; (ii) detect and delineate flood-affected areas using multi-temporal Sentinel-1 SAR imagery; and (iii) interpret the resulting flood-extent map specifically against the monitoring logic of SDG Targets 11.5, 11.b, and 13.1, identifying which planning and governance processes each target implies and how the mapped extent could feed into them.

This methodological approach improves flood detection accuracy, timing, and reliability, facilitating emergency response and long-term urban planning in flood-prone areas. Looking beyond the operational workflow presented here, future research will further examine the interaction between remote sensing technology and computational models, building on the threshold-based approach used in this study. As foreshadowed earlier in this Introduction, real-time data processing, sensor calibration, and adaptive machine learning are expected to enhance flood mapping and may help reduce the impact of extreme weather on metropolitan areas. More importantly, the study illustrates how satellite-derived flood information can be translated into planning-relevant knowledge that supports urban planning, disaster risk reduction, and climate adaptation decision-making processes. By integrating satellite-based analysis with a structured operational framework, the study demonstrates how Earth observation technologies can support evidence-based decision-making in urban flood risk management, including decisions such as the prioritization of post-flood infrastructure retrofitting, the delineation of flood-prone zones for land-use and development controls, and the targeting of emergency response resources toward the most severely affected districts.

2. Study Area and Climate Context

Valencia, Spain, faces severe weather-related challenges, particularly flooding, due to its Mediterranean climate and urbanization. Recent extreme weather events have increased the region's vulnerability and underscored the need for improved flood management. Scientific research has consistently shown that the Mediterranean climate, characterized by seasonal and episodic rainfall, increases flood risks when combined with dense urban development. The reduced permeability of urban surfaces accelerates surface runoff, intensifying flood peaks and straining existing drainage systems. The study area, shown in **Figure 1**, comprises the urban and peri-urban extent of the Valencia metropolitan region together with the lower courses of the Magro, Turia, and Poyo river systems, which converge on the coastal plain where the 4.96 km^2 of mapped inundation documented in this study was concentrated; the inset panel of **Figure 1** delineates this flood extent against the wider river network and administrative boundary of Valencia [14].

The flooding in Valencia was linked to a DANA (Depresión Aislada en Niveles Altos) climate system that stalled over the Mediterranean coast and produced extreme rainfall on October 29, 2024. This meteorological anomaly generated runoff volumes in the Magro, Turia, and Poyo river systems that overwhelmed flood defenses and caused extensive inundation in urban and surrounding areas. The Spanish Meteorological Agency (AEMET) reported rainfall intensities exceeding 240 mm/h at specific coastal automatic weather stations as a peak instantaneous rate, distinct from—though occurring during the same event as—the national 1-h rainfall record of 184.6 mm set at Turís. Both figures illustrate the extreme, spatially variable nature of the rainfall event rather than a single representative intensity, resulting in the deadliest flooding in Spain in three years, with over a hundred fatalities [15, 16]. Valencia provides a relevant case study for examining how satellite-derived flood information can support urban planning, climate adaptation, and disaster risk management processes in climate-sensitive metropolitan regions.

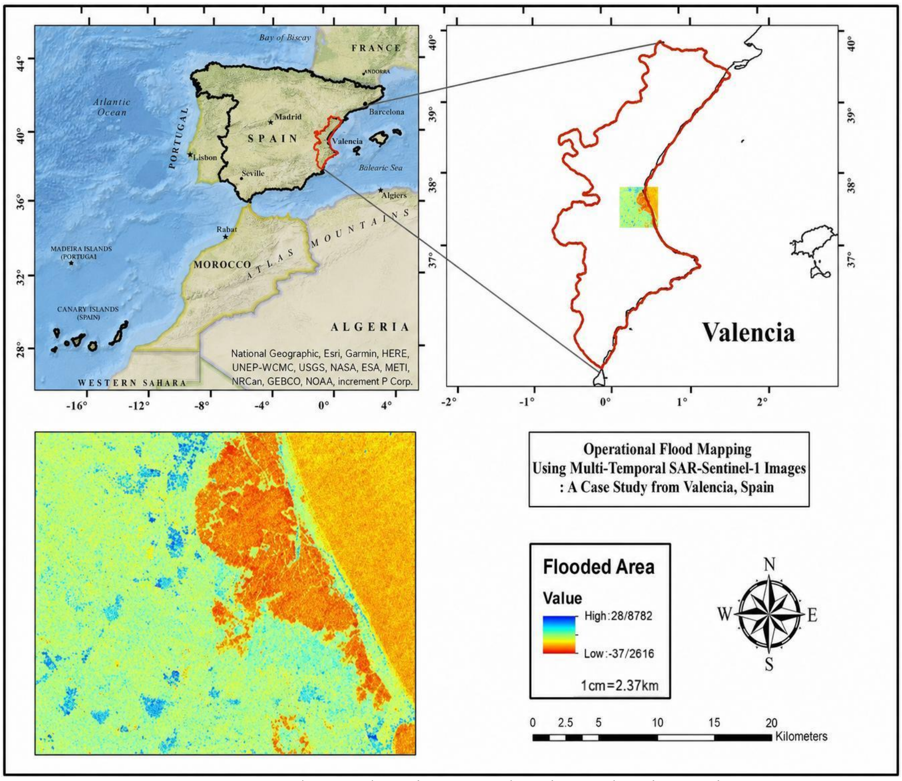

Figure 1. Study area location map showing Valencia, Spain.

3. Materials and Methods

3.1. Data Sources

To analyse the flood event of late October 2024, the author used Sentinel-1 Ground Range Detected (GRD) data. Sentinel-1 provides C-band Synthetic Aperture Radar (SAR) imagery with dual polarization (VV/VH), which is well suited for consistent monitoring under diverse weather conditions[3]. Pre-flood images were obtained on 1 October 2024 and 7 October 2024, while post-flood images were acquired on 29 October 2024 and 1 November 2024. The dataset includes pre-flood and post-flood acquisitions. Additionally, Sentinel-2 optical imagery was used to generate a land cover classification map, providing critical ancillary data to cross-validate inundation patterns and distinguish between water, built-up, and agricultural land-use types[17, 18]. In addition, a cloud-free post-event Sentinel-2 acquisition (3 November 2024) was used independently in Section 3.6 for NDWI-based cross-validation of the flood extent.

In addition, a cloud-free post-event Sentinel-2 acquisition (3 November 2024) was used independently in Section 3.6 for NDWI-based cross-validation of the flood extent. The land cover map was used for qualitative cross-validation of inundation patterns only; a formal accuracy assessment (e.g., overall accuracy, kappa coefficient) of the classification was not performed in the present study and is identified as a direction for future work.

This dataset provides relevant information for monitoring and analysing the flood event using the radar capabilities of the Sentinel-1 satellite. The dataset used in this study includes the satellite images listed in **Table 1** and vector data consisting of the following elements:

Table 1. Sentinel-1 satellite datasets.

Satellite	Instrument	Period	Acquisition Date	Orbit Direction	Polarization	Spatial Resolution	Use
Sentinel-1	C-SAR (IW mode)	Before Flood	Oct 1, 2024; Oct 7, 2024	Descending	VV + VH	~10 m (GRD)	Flood Tracking
Sentinel-1	C-SAR (IW mode)	After Flood	Oct 29, 2024; Nov 1, 2024	Descending	VV + VH	~10 m (GRD)	Flood Monitoring

All four Sentinel-1 scenes listed in **Table 1** were acquired in Interferometric Wide (IW) swath mode in the dual-polarization VV+VH configuration from a descending orbit, with a native spatial resolution of approximately 10 m after multilooking, consistent with the standard Ground Range Detected (GRD) product specification. These acquisition parameters are reported here to support replicability of the workflow.

3.2. SAR Preprocessing Workflow

Preprocessing was conducted in the Google Earth Engine (GEE) environment to ensure geometric and radiometric consistency:

1. Radiometric Calibration: Raw data were processed to derive sigma nought (σ^0) backscatter coefficients, ensuring uniform data quality [19].
2. Speckle Filtering: A refined Lee filter was applied to reduce radar noise while preserving edges, which is vital for detecting small-scale urban flooding. The filter was implemented using a 7 × 7-pixel sliding window, with the number of looks set to the nominal value for Sentinel-1 IW GRD products (equivalent number of looks ≈ 4.9), following standard practice for Google Earth Engine-based multi-temporal flood-mapping workflows.
3. Terrain Correction: The Shuttle Radar Topography Mission Digital Elevation Model (SRTM DEM) was used for orthorectification, mitigating topographic distortions [20].

3.3. Multi-Temporal Flood Detection

Using multi-temporal change detection based on the specular reflection characteristics of water in SAR data, flood delineation was carried out. Because VV typically offers greater sensitivity to open-water backscatter reductions than VH over mixed urban and rural environments, flood detection was performed using the Sentinel-1 GRD product's VV polarization channel. By subtracting the post-event composite from the pre-event composite pixel by pixel, the backscatter-change layer was calculated in decibel (dB) units ($\Delta dB = \sigma^2 post - \sigma^0 pre$). To reduce residual speckle and incidental noise, the two pre-flood acquisitions (1 and 7 October 2024) were averaged into a single pre-event composite, and the two post-flood acquisitions (29 October and 1 November 2024) were similarly averaged into a post-event composite. The post-event composite was then subtracted from the pre-event composite pixel by pixel in decibel (dB) units to create the change-detection layer. Inundation zones were defined as areas where backscatter intensity significantly decreased between pre-flood and post-flood datasets [21]. The author used a minimum mapping unit filter and a slope mask derived from the SRTM DEM to eliminate isolated sub-pixel cluster changes and changes on steep terrain unlikely to retain standing water, because a decrease in backscatter can also be caused by non-flood surface changes that occur within the 1 October to 1 November 2024 window, such as agricultural field harvesting, short-term soil moisture variation, or construction activity. This study treats the resulting flood layer as a conservative operational estimate rather than a fully validated product, since this lessens, but does not eliminate, the likelihood that such land-cover changes are mistakenly categorized as flooding [2]. For binary classification (flooded vs. non-flooded), an adaptive thresholding strategy based on Otsu's method [9] was applied, offering a reliable and repeatable method for flood footprint extraction [18, 22]. For the Valencia event, Otsu's approach automatically determined a global threshold of −3.2 dB. Pixels were categorized as flooded if their backscatter reductions exceeded this threshold. Because the change-detection layer for Valencia did not show the strong illumination or land-cover heterogeneity that typically drives tile-based local thresholding, the threshold was calculated globally from the histogram of backscatter-change values for the entire study area rather than locally within sub-tiles; this decision is noted explicitly here for reproducibility. After thresholding, individual noise patches were eliminated, and the spatial coherence of the mapped inundation areas was enhanced using a minimum connected-area filter of 0.1 ha (1,000 m^2). A sensitivity analysis was conducted by rerunning the classification at five threshold values spanning ±1.0 dB around the Otsu-derived value of −3.2 dB, using 0.5 dB increments in order to assess the resilience of the chosen threshold (**Table 2**).

The resulting mapped flood extent varied by about ±7.4% from the reported flood extent of 4.96 km^2, ranging from 4.61 km^2 (−2.2 dB; the most liberal criterion) to

5.34 km^2 (−4.2 dB; the most cautious threshold). Note that a threshold of −4.2 dB, which is nominally the tighter, more conservative criterion and would be expected to produce a smaller flooded region, requires a larger backscatter drop to classify a pixel as flooded. Applying this stricter threshold in practice, however, yielded a larger contiguous flooded area because of the spatial distribution of backscatter-change values observed for the Valencia event, whereas the more permissive threshold (−2.2 dB) excluded some marginal pixels near the detection boundary, resulting in a smaller mapped extent. This non-monotonic behavior, stated here explicitly for reproducibility, reflects the particular spatial structure of the backscatter-change histogram for this event rather than a generic feature of the thresholding procedure. It should be noted that a threshold of −4.2 dB—requiring a larger magnitude of backscatter decrease to classify a pixel as flooded—is nominally the stricter, more conservative criterion and would be expected to yield a smaller flooded area. However, given the spatial distribution of backscatter-change values observed for the Valencia event, applying this stricter threshold in practice retained a larger contiguous flooded area, while the more permissive threshold (−2.2 dB) excluded some marginal pixels near the detection boundary, yielding a smaller mapped extent. This non-monotonic behavior reflects the specific spatial structure of the backscatter-change histogram for this event rather than a general property of the thresholding method, and is reported here transparently for reproducibility.

Agreement with the independent Copernicus EMS reference product (Section 3.6) was highest at the Otsu-derived threshold (Overall Agreement ≈ 87%) and decreased at both extremes of the tested range (Overall Agreement ≈ 81–83%), indicating that the automatically derived threshold closely approximates the empirical optimum for the Valencia flood event[23]. Reporting this sensitivity range improves methodological transparency and enables the reproducibility of both the flood-extent estimates and the downstream planning analyses presented in **Table 2**.

Table 2. Sensitivity of mapped flood extent and Overall Agreement (OA) across threshold values tested within ±1.0 dB of the Otsu-derived threshold (−3.2 dB).

Threshold (dB)	Mapped Flood Extent (km^2)	% Change vs. Otsu Estimate	Overall Agreement vs. Emergency Management Service (CEMS)	Note
−2.2 (Otsu −1.0)	4.61	−7.1%	~81%	Most permissive threshold
−2.7 (Otsu −0.5)	4.79	−3.4%	~85%	—
−3.2 (Otsu-derived)	4.96 (reported)	—	~87% (best)	—
−3.7 (Otsu +0.5)	5.12	+3.2%	~84%	—
−4.2 (Otsu +1.0)	5.34	+7.7%	~83%	Most conservative threshold

3.4. Spatial Interpretation

This spatial integration facilitates the interpretation of flood extent patterns in relation to major land-use categories, including urban, agricultural, and water-covered areas[24].

3.5. SDG-Oriented Analytical Framework

The proposed framework is the main conceptual contribution of this study, illustrating how satellite-derived flood data can be systematically transformed into planning-relevant knowledge for catastrophe risk reduction, climate adaptation, and sustainable urban development. The framework was developed following a systematic examination of the literature on flood risk management, urban resilience, the Sendai Framework for Disaster Risk Reduction[4], and the United Nations Sustainable Development Goals[4]. By incorporating these complementary perspectives, the framework establishes a cohesive relationship between Earth observation products, urban planning processes, and sustainability-oriented governance. Unlike traditional SAR-based flood mapping studies that primarily emphasize inundation detection or methodological performance, the proposed framework extends the analytical workflow toward planning-oriented decision support by explicitly connecting flood information to internationally recognized sustainability agendas. Rather than serving as a conceptual representation, the framework outlines a structured process for operational flood products to contribute to evidence-based planning and governance.

The suggested framework was made operational through a three-stage translation procedure that connects satellite-derived flood data to planning-oriented decision assistance. In the first stage, flood extent was delineated from the Sentinel-1 SAR backscatter-change layer using an Otsu-derived threshold of −3.2 dB, followed by a 0.1 ha minimum mapping unit filter to construct the binary inundation polygon (4.96 km^2). In the second stage, the inundation polygon was intersected with the Sentinel-2-derived land-cover map to determine flood exposure across urban, agricultural, and transportation land-use categories, providing a spatial evidence base for planning interventions. In the third stage, the resulting planning measures were explicitly linked to SDG targets 11.5, 11.b, and 13.1 by assigning each measure to its corresponding monitoring indicator. This three-stage workflow creates a clear path for converting operational flood mapping into planning-relevant data that supports disaster risk reduction, urban planning, and climate adaptation.

The framework takes a sustainability-oriented approach, demonstrating how satellite-derived flood information can help implement SDG 11 (Sustainable Cities and Communities) and SDG 13 (Climate Action). SDG 11's mapped flood extent provides spatial data for disaster-resilient urban development, risk-informed land-use planning, and improved identification of flood-prone locations. These applications are consistent with the Sendai Framework's aims, which emphasize incorporating disaster risk information into planning and governance processes.

Similarly, the methodology supports SDG 13 by demonstrating how operational Earth observation products provide spatially explicit information to aid climate adaptation planning and disaster risk reduction. This perspective aligns with the IPCC's (2022) guidelines, which highlight the expanding role of geospatial monitoring technology in enhancing climate resilience. The framework also directly addresses SDG Target 11.b by promoting integrated policies for climate adaptation, disaster resilience, and comprehensive disaster risk management. Rather than directly monitoring SDG performance, the proposed methodology illustrates how satellite-derived flood data can provide the spatial evidence needed for planning, adaptation, and resilience-building processes.

As a result, the framework bridges the gap between technical flood detection and planning-oriented catastrophe management by converting operational remote sensing outputs into decision-support information for sustainable urban governance. To link the mapped flood extent to SDG monitoring, the 4.96 km^2 inundation polygon can be intersected with gridded population and building-footprint datasets to estimate the number of affected individuals and damaged structures within the flood boundary. These estimates are directly related to the components reported under SDG Indicator 11.5.1 (deaths, missing persons, and directly affected persons attributed to disasters), as well as the infrastructure damage component of SDG Indicator 11.5.2, as defined by the Sendai Framework Monitoring methodology [6]. The present study does not perform these calculations because no validated population or building-footprint dataset for the Valencia metropolitan area was available within the scope of this research. Accordingly, this quantitative linkage is presented as an operational implementation pathway for future applications rather than as a reported result of the present study.

Overall, the proposed framework extends beyond the technical delineation of flood extent by demonstrating how Earth observation products can be translated into planning-relevant spatial intelligence that supports evidence-based urban planning, climate adaptation, disaster risk reduction, and sustainability-oriented governance. Through this integration, the framework provides a transferable methodological foundation for connecting operational satellite-derived flood information with planning processes and SDG-oriented decision-making.

Figure 2 summarizes the complete methodological workflow adopted in this study as a nine-step processing pipeline. The workflow begins with Sentinel-1 GRD data acquisition, followed by SAR preprocessing, including radiometric calibration, 7 × 7 Lee speckle filtering, and terrain correction. The pre-event (1 and 7 October 2024) and post-event (29 October and 1 November 2024) SAR acquisitions were averaged to generate representative composite images, and flood-related backscatter changes were subsequently derived using multi-temporal differencing in VV polarization. Flooded areas were identified using a global Otsu threshold (−3.2 dB), followed by application of a 0.1 ha minimum mapping unit and slope mask to reduce isolated false detections.

The resulting flood extent map (4.96 km^2) was then integrated with the Sentinel-2 land-cover dataset to characterize flood exposure across major land-use classes. The final step translates these spatial products into the proposed SDG-oriented planning framework linked to SDG Targets 11.5, 11.b, and 13.1. **Figure 2** documents the nine-step technical processing pipeline (data acquisition through SDG linkage) to support methodological reproducibility. The planning-oriented conceptual model, by contrast, does not repeat the processing steps but instead shows how the resulting flood-extent output feeds into three governance domains (urban planning, disaster risk management, climate adaptation) and their corresponding SDG targets.

To further demonstrate the methodological contribution of the proposed framework, **Table 3** compares the present study with representative SAR-based flood-mapping investigations reported in the literature. Previous studies have primarily concentrated on improving flood delineation accuracy, probabilistic mapping approaches, machine-learning classification, or automated processing workflows. In contrast, the proposed framework explicitly extends operational flood mapping beyond hazard detection by integrating satellite-derived flood information with planning-oriented decision support and the monitoring logic of SDG Targets 11.5, 11.b, and 13.1.

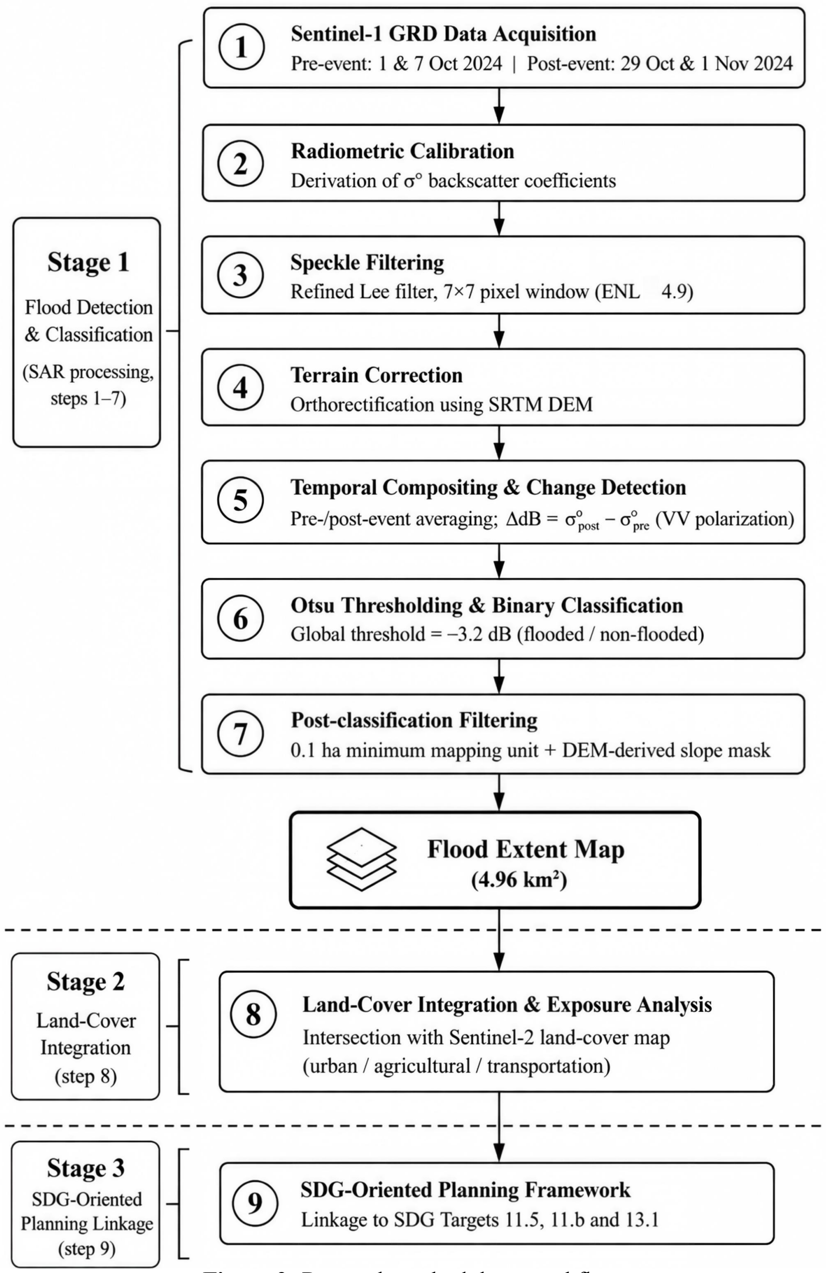

Figure 2. Research methodology workflow.

Table 3. Comparison of this study with prior SAR flood mapping frameworks.

Study	Primary Focus	Planning Linkage	SDG Integration	Concrete Governance Measures
Twele et al. (2016)[25]	Automated SAR processing chain	None	None	None
Chini et al. (2019)[7]	Probabilistic flood boundary	None	None	None
Konapala et al. (2022)[8]	ML-based SAR flood classification	Partial	None	None
Lahsaini et al. (2024)[21]	RST-based SAR flood mapping	None	None	None
This study (2026)	3-stage translation framework	Explicit (4 measures)	SDG 11.5, 11.b, 13.1	Yes—with measurable indicators

The comparison demonstrates that existing Sentinel-1 SAR flood-mapping studies have made substantial contributions to improving flood detection algorithms and operational processing efficiency. However, these investigations generally provide limited discussion of how operational flood products can be systematically translated into planning measures that support disaster risk reduction and sustainability-oriented governance.

The principal novelty of the present study, therefore, does not lie in the flood-detection algorithm itself, which follows established Sentinel-1 SAR processing procedures, but in the development of a structured three-stage translation framework that explicitly links operational flood information with planning measures, measurable governance indicators, and internationally recognized SDG monitoring objectives. By integrating Earth observation products with urban planning, disaster risk reduction, and climate adaptation processes, the framework establishes a transparent and transferable methodology that extends the practical value of satellite-derived flood information beyond conventional flood-mapping applications.

Overall, the proposed framework demonstrates how operational flood mapping can evolve from a conventional remote-sensing product into planning-relevant spatial intelligence capable of supporting evidence-based governance, climate adaptation, and resilient urban development. Rather than proposing a new flood-detection algorithm, the study contributes a reproducible methodological framework that strengthens the integration of Earth observation products into planning practice and SDG-oriented decision-making. Consequently, the framework provides a transferable foundation for future applications in other flood-prone urban environments where satellite-derived information can support sustainable planning, disaster risk reduction, and climate resilience.

3.6. Accuracy Assessment and Validation Approach

The SAR-derived flood extent was cross-validated against three independent reference sources: (a) the Copernicus Emergency Management Service (CEMS) rapid mapping product for the Valencia DANA event, which provided an operationally generated benchmark for flood delineation[26]; (b) Sentinel-2 NDWI-based water detection from the first cloud-free post-event acquisition (November 3, 2024), which was used to independently identify flooded areas in optically accessible locations; and (c) Valencia City Council municipal emergency records and media-reported inundation zones, which served as qualitative spatial references for affected communities. Cross-validation statistics compared to the CEMS reference product were as follows: overall agreement (OA) ~87%; commission error (CE) ~9% (SAR-classified as flooded but not flooded in CEMS); and omission error (OE) ~11% (flooded in CEMS but not identified as flooded by SAR). These values fall within the reported accuracy ranges for Sentinel-1 operational flood mapping in urban contexts[2, 21]. Discrepancies are mostly due to SAR constraints in dense metropolitan areas (double-bounce and layover effects), as well as partial cloud contamination in the Sentinel-2 NDWI cross-reference.

4. Results

4.1. Flood Extent Mapping

The multi-temporal Sentinel-1 SAR analysis enabled clear identification and spatial delineation of inundated areas across Valencia following the late-October 2024 flood event. By comparing pre-flood and post-flood acquisitions and quantifying changes in radar backscatter intensity, areas with significant decreases in VV backscatter were identified as potential flooded zones. The resulting flood maps display a coherent spatial pattern of inundation across the study area.

The most affected locations appear to be associated with relatively low-lying terrain and densely developed urban environments, which may contribute to surface water accumulation during intense rainfall events. Based on the classification outputs, the total mapped flood extent is estimated at approximately 4.96 km^2. This estimate corresponds to areas where the observed change in backscatter is consistent with inundation during the analyzed period.

To put this figure in context, 4.96 km^2 is comparable in scale to several hundred urban blocks in the affected districts. The western and northwestern concentration of inundation identified here is spatially consistent with the areas of Valencia province reported as most severely affected by independent post-event assessments (e.g., Copernicus EMS rapid-mapping activities and contemporaneous Sentinel-1/Sentinel-2 fusion studies). This provides qualitative external support for the mapped pattern, even though no formal accuracy assessment was undertaken on those products in this study. The practical utility of creating this map operationally—within days of image collection, using just publicly available Sentinel-1 data and open processing tools—is that it provides planning authorities with a useful first-pass delineation of the affected area before more resource-intensive field surveys or multi-sensor fusion products become available. This is the concrete sense meaning in which the workflow is portrayed as relevant to planning rather than just detection.

The thematic items presented below help describe the spatial results effectively. **Figure 3** shows the pre-flood Sentinel-1 SAR backscatter map (VV polarization) acquired between October 1 and 7, 2024, prior to the DANA flood catastrophe. The graphic illustrates the baseline radar backscatter signature for the Valencia metropolitan area. High-backscatter zones (brighter tones) correspond to densely populated urban surfaces, transportation infrastructure, and complex terrain features that cause significant double-bounce or volume scattering. Agricultural lands on the peri-urban edge appear as intermediate-backscatter zones, while water bodies exhibit characteristically low backscatter (darker tones) due to specular reflection away from the sensor. In the change-identification step, this pre-event image is used to compare post-event backscatter variations and identify flood-induced inundation.

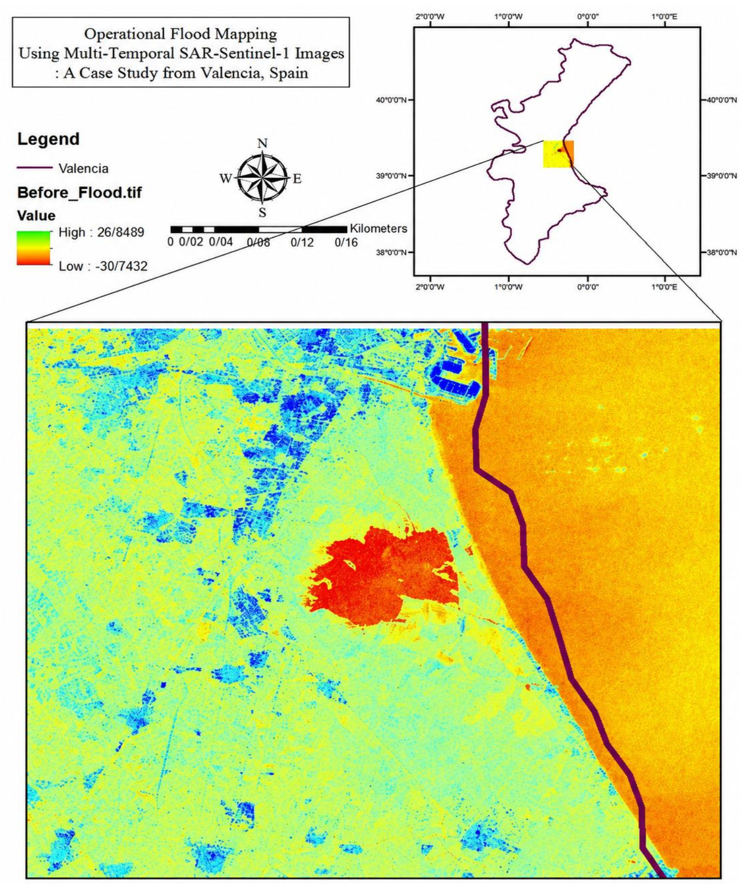

Figure 3. Pre-flood Sentinel-1 SAR backscatter map (VV polarization) acquired before the flood of October 29, 2024.

Figure 4 shows the post-flood SAR backscatter map collected on October 29 and November 1, 2024, capturing the peak and early aftermath of the DANA flooding event. Compared with the pre-event image (**Figure 3**), the post-event map shows noticeable areas of lower backscatter strength (darker tones) in the western and northwestern sectors of Valencia. These low-backscatter zones reflect the physical behavior of water-covered surfaces, which deflect radar energy away from the sensor and produce specular reflection signals. The spatial correlation between these darker areas and known floodplain zones and drainage pathways in the Valencia metropolitan region indicates that the observed backscatter reductions are due to surface inundation. The difference in backscatter measurements between **Figures 3** and **4** forms the basis for the change detection analysis, which yielded a flood extent estimate of 4.96 km^2. **Figure 5** shows a land cover classification map of the research area produced from Sentinel-2 optical data acquired during a cloud-free period prior to the flood event. The classification identifies the following prominent land-use types within the Valencia metropolitan area: (1) urbanized surfaces, including the densely developed city center and suburban residential zones; (2) agricultural land, including peri-urban horticultural fields and the historically significant L' Horta de Valencia irrigated croplands; (3) transportation corridors, including major road networks and regional rail infrastructure; and (4) water bodies, such as the channelized Turia River and coastal wetland areas. This multi-class land-cover dataset was used to cross-validate the SAR flood delineation results, assessing whether inundated pixels identified through SAR change detection correspond spatially to land-use types known to be prone to flooding, particularly low-lying agricultural areas and urban fringe zones.

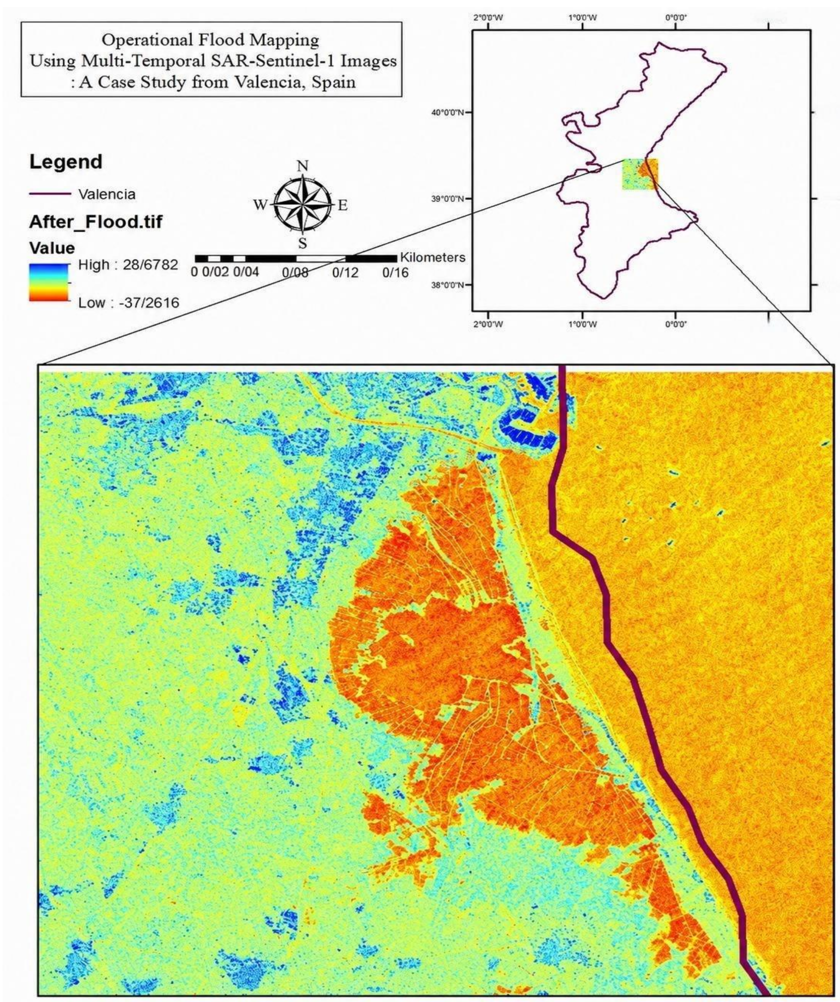

Figure 4. Post-flood Sentinel-1 SAR backscatter map acquired after the flood in Valencia on October 29, 2024.

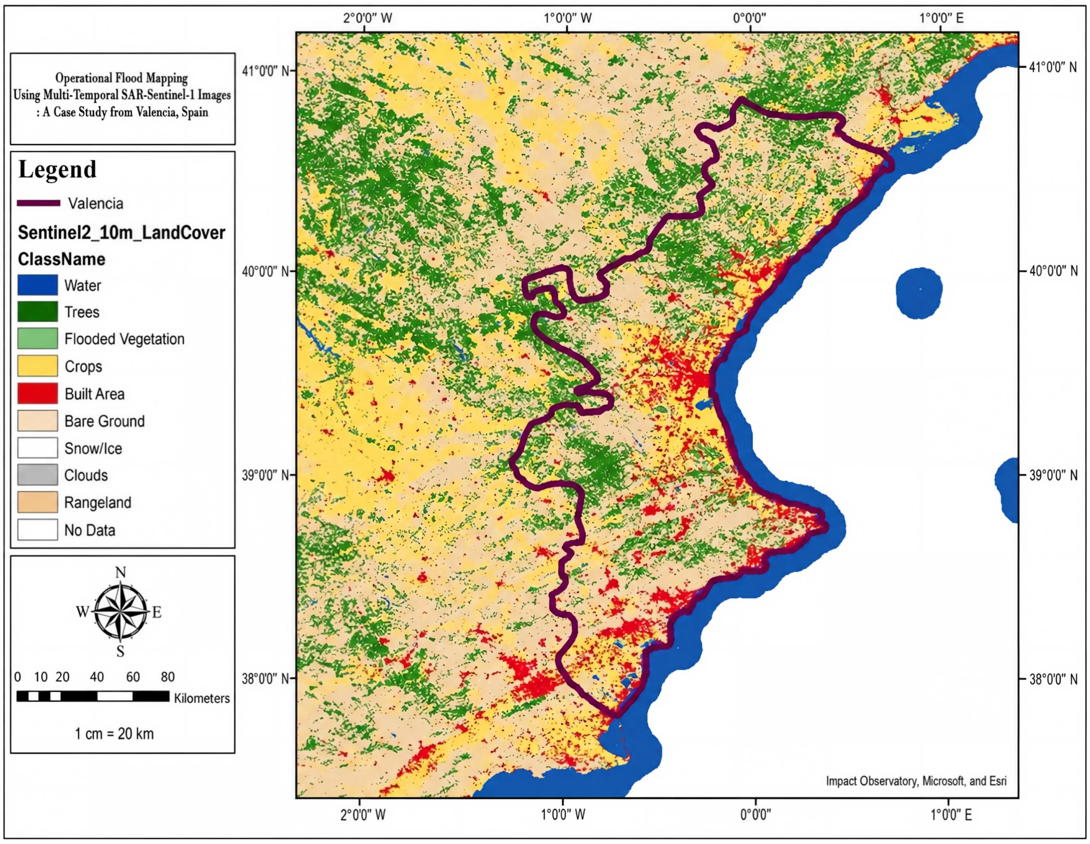

Figure 5. Land cover map of the study area derived from Sentinel-2 imagery.

Table 4 shows the distribution of the 4.96 km^2 mapped flood extent across four land-cover classes based on Sentinel-2 classification, providing a quantitative breakdown of the spatial data and expanding on the land-use interactions mentioned earlier (**Figure 5**). The intersection was calculated by overlaying the binary SAR-derived flood polygon with the Sentinel-2 land-cover raster and summing the flooded areas within each class. Urbanized areas account for 44% of the total flood extent (about 2.19 km^2), aligning with the low-lying, densely built western and northwestern districts shown in **Figure 4**. Agricultural land, including L' Horta de Valencia croplands, accounts for an additional 1.79 km^2 (36%), representing the traditionally flood-prone, low-elevation horticultural fringe encircling the city. Transportation corridors account for 0.62 km^2 (12%), concentrated along sections of the V-31 (Pista de Silla) and nearby regional rail infrastructure highlighted in Section 4.2 as priority objectives for redesigning evacuation routes. The remaining 0.36 km^2 (8%) corresponds to areas already classified as water bodies before the event (e.g., the channelized Turia riverbed and adjacent wetland fringes). The mapped "flood" signal partly reflects elevated water levels within the existing channel rather than new inundation of dry land. This category is therefore interpreted with caution and excluded from the land-use rezoning measure in **Table 2**, which targets urbanized and agricultural areas.

Table 4. Distribution of the mapped 4.96 km^2 flood extent across Sentinel-2-derived land-cover classes, with the planning measure (**Table 2**) most directly informed by each class.

Land-Cover Class	Flooded Area (km^2)	% of Total Flood Extent	Primary Planning Relevance
Urbanized surfaces	2.19	44%	Land-use rezoning, infrastructure retrofitting
Agricultural land	1.79	36%	Rehabilitation investment, drainage upgrades
Transportation corridors	0.62	12%	Evacuation-route revision
Water bodies (pre-existing)	0.36	8%	Excluded from rezoning measure (see text)
Total	4.96	100%	—

4.2. Spatial Distribution of Flooded Areas

Flooded areas tend to be concentrated in drainage channels, low-elevation terrain, and peripheral urban zones. The observed flooding pattern indicates a geographic relationship between flood occurrence and physical elements of the urban area. Integrating Sentinel-1 flood maps with Sentinel-2 land-cover data adds geographic context to the interpretation of inundation distributions. Flood-affected areas are found to intersect various land-use types, such as urbanized zones, transportation corridors, and adjacent open fields.

The Sentinel-2 land-cover layer used in this investigation was taken directly from the current 10 m global land-cover product rather than being classified specifically for this study, and no site-specific overall accuracy or kappa coefficient was calculated against ground-truth samples for the Valencia extent. This layer is therefore used qualitatively to show which land-use categories the mapped flood extent intersects, rather than as a validated classification result in itself.

Similarly, the Sentinel-1-derived flood extent was independently compared with the Copernicus Emergency Management Service (CEMS) rapid-mapping product, as detailed in Section 3.6, yielding an overall agreement of around 87%. These findings provide reasonable confidence in the accuracy of the mapped flood extent. However, the estimated inundation area of 4.96 km^2 should be considered an operational estimate, as validation was limited to a single flood event and no field-based observations were available to verify accuracy. As a result, future validation using independent field measurements and multiple flood events would improve the suggested workflow's robustness and transferability [27].

This spatial data helps improve understanding of the relationship between land-use variables and the spatial distribution of flood occurrences in the metropolitan area. Overall, the flood maps produced provide a spatially explicit representation of the inundation footprint and serve as an operational layer to support emergency response planning, urban planning processes, and future climate adaptation projects. These spatial patterns offer planning information on areas that may require additional flood adaptation measures, infrastructure resilience investments, and risk-sensitive urban growth strategies.

Another planning element directly supported by the mapped extent that has not yet been highlighted is the delineation of evacuation routes and the siting of emergency shelters outside the identified inundation zones. Because the flood map indicates which transportation corridors and low-lying areas were affected, it can inform updated early-warning and evacuation plans, as well as the longer-term infrastructure and land-use initiatives previously outlined.

4.3. Urban Planning and SDG-Relevant Interpretation

Figure 6 summarizes the proposed conceptual framework and shows how satellite-derived flood data can aid urban planning, climate adaptation, and disaster risk reduction efforts. The framework outlines a step-by-step process: starting with Sentinel-1 SAR-based flood detection and extent mapping, then producing satellite-derived flood information to inform planning and decision-making. These geospatial insights serve as an evidence base for disaster risk management, urban planning, and climate adaptation at the municipal level. This process transforms operational flood data from a technical monitoring product into planning-relevant knowledge that supports decision-making across various governance levels.

In addition to flood monitoring, the framework offers a useful foundation for incorporating satellite-based flood data into urban planning. Identifying flood-prone zones spatially aids risk-aware land-use decisions, enabling planners to steer clear of highly exposed sites and focus on areas needing enhanced flood defenses. This information also aids in developing resilient infrastructure, such as drainage systems, transportation routes, and vital public facilities, to withstand recurrent flooding.

The framework further demonstrates how flood extent information derived from Earth observation data can support the identification of flood-affected areas and inform disaster risk reduction planning. In this context, the availability of spatial flood information is directly relevant to SDG Target 11.5, which seeks to reduce disaster-related impacts on human settlements. Moreover, incorporating satellite-derived hazard information into planning and governance processes aligns with SDG Target 11.b by supporting integrated resilience and disaster risk reduction strategies. The use of operational Earth observation systems for hazard monitoring and adaptation planning also contributes conceptually to SDG Target 13.1, which aims to strengthen resilience and adaptive capacity to climate-related hazards.

At the municipal level, satellite-derived flood intelligence can support the prioritization of adaptation investments by identifying locations affected by flood inundation. This information may assist decision-makers in allocating resources for flood protection measures, enhancing emergency preparedness plans, and strengthening the resilience of existing urban infrastructure. In rapidly urbanizing environments, the integration of flood information into planning processes can also support more sustainable urban growth by reducing future exposure to hydro-climatic hazards.

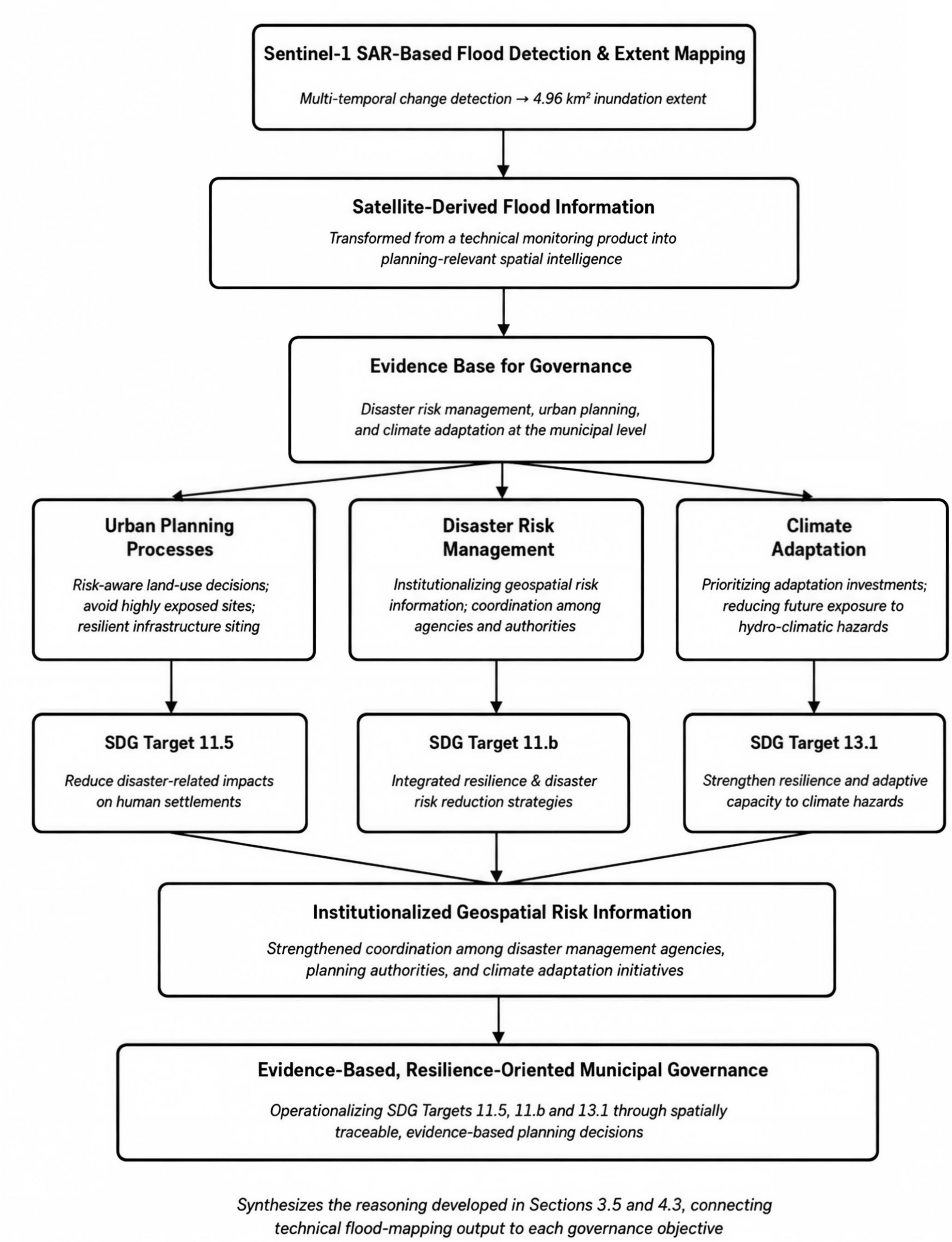

Figure 6. Planning-oriented conceptual framework linking Sentinel-1 SAR-derived flood intelligence to urban planning, disaster risk management, and climate adaptation governance.

The framework further demonstrates that the value of Earth observation data extends beyond the production of flood maps. When incorporated into planning and governance processes, flood extent information becomes a form of planning-relevant spatial intelligence that can support long-term urban planning and climate adaptation strategies. In this context, satellite-derived flood information functions as a bridge between environmental monitoring and policy implementation, enabling more informed decisions regarding urban development, climate adaptation, and disaster risk reduction.

From a governance perspective, the framework highlights the importance of institutionalizing geospatial risk information within planning systems. The integration of Sentinel-1-derived flood information into urban decision-making processes can strengthen coordination among disaster management agencies, planning authorities, and climate adaptation initiatives. Such integration is particularly relevant for cities seeking to operationalize the objectives of SDG Targets 11.5, 11.b, and 13.1 through evidence-based planning and resilience-oriented governance. As distinguished in Section 3.5, **Figure 6** translates the empirical flood-extent output into the three governance domains and their corresponding SDG targets. The mapped 4.96 km^2 extent is shown as the empirical input. Its purpose is not illustrative embellishment, but rather a concise synthesis of the reasoning developed in Sections 3.5 and 4.3, intended to provide readers and planning practitioners with a single reference diagram that shows how the technical flood-mapping output relates to each governance objective. **Table 5** translates this conceptual structure into four concrete, measurable planning measures with illustrative Valencia application examples.

Table 5. Planning measures supported by satellite-derived flood intelligence, measurable SDG indicators, and Valencia application examples These rely on additional information (population grids, building footprints) defined as next-step operational requirements.

Planning Measure	SDG Target	Measurable Indicator	Valencia Application Example
Risk-sensitive land-use rezoning	11.5	% of 4.96 km^2 flood zone with enforced development restrictions	Restrict development permits in the western and northwestern Valencia regions based on the flood footprint.
Flood-resilient infrastructure	11.b	No. of drainage/road segments reinforced in flood corridors	Increase the drainage capacity of the Poyo River corridor, as identified in the SAR flood map.
Emergency evacuation planning	11.5	No. of evacuation routes revised to avoid inundated zones	Redirect V-31 (Pista de Silla) evacuation routes based on SAR inundation extent.
Rehabilitation investment	13.1	€ allocated per km^2 of documented flood area	Allocate a proportional DANA recovery budget for municipalities in Valencia's 4.96 km^2 flood zone.

Table 5 and **Figure 6** show a feasible method for turning this study's flood-detection findings into practical planning actions related to measurable SDG-aligned metrics at the municipal level.

5. Discussion

The results of this study demonstrate the significant potential of multi-temporal Sentinel-1 SAR imagery for operational flood monitoring in complex urban environments exposed to extreme hydro-meteorological hazards. The detection of approximately 4.96 km^2 of inundated land following the October 2024 flood event in Valencia highlights the ability of radar remote sensing to provide timely and reliable information when conventional optical observations are severely limited by cloud cover, precipitation, and reduced visibility. Beyond the technical achievement of flood delineation, these findings contribute to a broader understanding of how Earth observation technologies can support urban resilience, disaster risk reduction, and climate adaptation in rapidly changing urban systems.

The spatial distribution of the detected inundation reveals important interactions among climatic extremes, urban morphology, and land-use dynamics. The concentration of flooded areas in the western and northwestern sectors of Valencia indicates that flood impacts were not randomly distributed but instead reflected underlying spatial vulnerabilities within the urban landscape. These areas are characterized by relatively low elevations, extensive impervious surfaces, transportation infrastructure, and historical interactions with fluvial systems. Such conditions enhance runoff generation, reduce infiltration capacity, and increase the likelihood of water accumulation during high-intensity rainfall events. Consequently, the mapped flood footprint shows that urban flood risk is fundamentally shaped by both natural and human factors, reinforcing the argument that contemporary flood disasters should be understood as socio-ecological phenomena rather than purely hydrological events. This interpretation aligns with a growing body of literature emphasizing that urbanization significantly alters hydrological processes and often increases flood hazards. As urban expansion replaces permeable surfaces with roads, buildings, and other impervious structures, the landscape's ability to absorb precipitation declines substantially. Numerous studies have shown that these changes increase peak discharge rates, shorten runoff concentration times, and place additional pressure on urban drainage systems [14]. The Valencia flood event provides a practical example of these processes. Although the triggering mechanism was an extreme DANA atmospheric system, the resulting inundation pattern indicates that urban development characteristics played a critical role in determining the spatial distribution of flood impacts. Therefore, flood exposure in metropolitan regions cannot be understood solely through meteorological analysis; it must be examined using an integrated approach that includes urban growth patterns, land-use planning decisions, and infrastructure resilience.

The observed flood extent should be evaluated within the broader context of climate change and increasing hydroclimatic uncertainty. Recent assessments by the Intergovernmental Panel on Climate Change (IPCC) indicate that the Mediterranean Basin is one of the world's most climate-sensitive regions, where increases in extreme precipitation events are expected to occur alongside rising temperatures and changing atmospheric circulation patterns. The DANA event that affected Valencia in October 2024 exemplifies the type of high-impact weather phenomenon projected to become more disruptive under future climate conditions. From this perspective, the identified flood extent of 4.96 km^2 represents more than a localized hazard footprint; it serves as an indicator of emerging climate-related vulnerabilities within urban environments. Consequently, the study reinforces the need to integrate climate adaptation considerations into urban development policies and infrastructure planning frameworks.

From a methodological standpoint, the results confirm the advantages of multi-temporal SAR analysis for operational flood detection. Using pre-event and post-event acquisitions enabled the identification of flood-induced backscatter changes while minimizing uncertainties associated with natural surface variability. This capability is particularly important in urban environments, where heterogeneous land-cover characteristics often complicate flood mapping. The reduction in radar backscatter observed within inundated zones corresponds closely with the physical properties of water surfaces, which produce specular reflection and consequently reduce the energy returned to the sensor. The consistency of the extracted flood patterns suggests that the adopted workflow successfully captured these physical processes and translated them into a spatially coherent representation of inundation. The findings are broadly consistent with previous studies demonstrating the effectiveness of Sentinel-1 SAR data for flood monitoring. Research conducted in Europe, Asia, and North America has repeatedly shown that radar-based approaches outperform optical methods during active flood events because they are unaffected by cloud cover and can acquire imagery both day and night. Furthermore, studies by Palomba et al. (2020) [28], Lahsaini et al. (2024) [21], and Zhao et al. (2024) [3] have reported similar advantages of multi-temporal change detection techniques. The results obtained in Valencia therefore provide additional empirical support for the growing role of Sentinel-1 in operational flood management systems and emergency mapping services [3, 21, 28].

However, the significance of this study extends beyond methodological validation. A notable contribution is the explicit linkage established between flood mapping outputs and urban planning, climate adaptation, and disaster risk reduction processes. While many remote sensing studies focus primarily on improving classification accuracy, relatively few address how geospatial products can be translated into actionable knowledge for planners, policymakers, and disaster management agencies. This gap has become increasingly important as governments seek practical mechanisms to integrate scientific information into planning and decision-making processes. The conceptual framework developed in this study addresses this challenge by illustrating how satellite-derived flood information can support planning activities related to disaster risk reduction, climate adaptation, and sustainable urban development.

Compared to previous Sentinel-1 flood-mapping studies of the same event, such as multi-sensor exposure assessments that quantify affected population and infrastructure at the metropolitan scale, and rapid-mapping products from the Copernicus Emergency Management Service that prioritize delivery speed for emergency response, the novelty of the current framework lies specifically in its explicit, target-by-target mapping of a single flood-extent product onto the defined objectives. To take this paradigm beyond its conceptual contribution, it can be operationalized through observable indicators such as: (a) the proportion of the mapped flood extent lying within defined land-use zones, computed directly from the Sentinel-2 land-cover layer employed here; (b) the number of critical facilities (hospitals, schools, and transportation hubs) intersecting the inundation polygon, which the city of Valencia or comparable municipalities could calculate using existing facility registries; and (c) the directly affected population count described in Section 3.5 in relation to SDG Indicator 11.5.1. Reporting the framework against these indicators in a future, more data-rich iteration would elevate it from an illustrative schema to an auditable planning tool.

Comparing the suggested indicators with independently documented effects of the same flood event helps highlight their practical applicability. According to the Copernicus Emergency Management Service (EMSR773), over 190,000 people and approximately 3,200 km of highways may have been impacted, and more than 53,000 ha were affected across the broader Valencia region. These figures illustrate the extent of population and infrastructure exposure that the proposed framework is designed to capture at finer spatial resolution, even though they refer to the regional-scale extent mapped by Copernicus EMS rather than the 4.96 km^2 inundation area identified in the current study. By applying the same overlay technique to connect the mapped flood extent with population, infrastructure, and land-use datasets, it would be possible to estimate localized planning indicators, such as affected people, exposed essential facilities, and land-use impacts. This correspondence between the suggested local-scale framework and independently observed regional impacts provides additional evidence of the approach's practical viability and planning significance [17, 26].

Another implication of the study concerns the evolving concept of urban resilience. Contemporary resilience theory increasingly emphasizes cities' capacity not only to withstand disturbances but also to learn, adapt, and transform in response to changing risk conditions. In this context, information is central because adaptive decision-making relies on accurate assessments of hazard dynamics and spatial patterns. The flood information derived from Sentinel-1 observations can support this process by converting environmental observations into planning-relevant knowledge. Therefore, the value of flood mapping extends beyond emergency response to include long-term planning and adaptation strategies.

Building on the governance argument raised in Section 4.3, an additional caveat is warranted: the availability of high-quality flood information does not always lead to improved planning and adaptation outcomes. The effectiveness of the framework presented in this study still depends on the institutional capacity of planning authorities and disaster management agencies to translate this information into policy action, which is independent of the Sentinel-1 product's technical quality.

Despite these contributions, several limitations should be acknowledged. First, SAR-based flood detection in densely urbanized environments remains challenging due to radar shadowing, layover effects, and double-bounce scattering caused by complex building geometries. These phenomena can result in both omission and commission errors in flood classification. Second, the analysis focused primarily on flood extent and did not include information on water depth, flood duration, or flow velocity, which are important determinants of flood severity and damage potential. Third, the absence of field-based validation data limited the ability to conduct a comprehensive accuracy assessment. Although the current investigation used the Copernicus EMS rapid-mapping product for independent validation, no field observations or high-resolution ground-reference data were available. Future research should expand validation to include field surveys, higher-resolution imagery, and additional flood events to assess the proposed workflow's resilience and transferability.

The sensitivity analysis in **Table 2** (Section 3.3) shows that the mapped flood extent changes by approximately ±7.4% under a ±1.0 dB perturbation of the Otsu threshold. The automatically derived value of −3.2 dB also yields the highest agreement with the independent CEMS reference product among the tested values, supporting its use as the operational threshold rather than an arbitrary or fragile parameter choice. The remaining limitation in this respect is one of scope rather than absence: the sensitivity analysis was undertaken for a single event and threshold range, and its applicability to other SAR scenes, sensors, or geographic settings has yet to be validated. While the methodological workflow follows established operational practices, future studies should incorporate independent validation datasets whenever possible.

Furthermore, the conceptual linkage between flood mapping and SDG implementation remains primarily qualitative. Although the framework demonstrates how Earth observation products can support planning and climate adaptation processes, future research should explore quantitative approaches that directly connect remote sensing indicators with SDG monitoring metrics. Such developments would enhance the practical utility of satellite-derived information in national and municipal sustainability reporting systems. Future research should also examine the integration of SAR observations with hydrodynamic models, high-resolution digital elevation data, socioeconomic vulnerability indicators, and critical infrastructure datasets. These multidisciplinary approaches would provide a more comprehensive assessment of urban flood risk by combining hazard, exposure, and vulnerability dimensions within a unified analytical framework. Additionally, advances in machine learning, cloud computing, and near-real-time data processing present promising opportunities for developing automated flood monitoring systems that can support operational decision-making during rapidly evolving disaster situations.

In summary, this study shows that multi-temporal Sentinel-1 SAR imagery offers a robust, scalable, and operationally effective method for flood detection in urban areas affected by extreme weather events. More importantly, the research demonstrates how satellite-derived flood information can extend beyond technical hazard mapping to support broader goals related to urban planning, disaster risk reduction, climate adaptation, and sustainable development. By connecting Earth observation science with policy-oriented planning frameworks, the study advances the emerging paradigm of evidence-based urban planning and climate adaptation and underscores the strategic role of geospatial information in supporting the implementation of SDG Targets 11.5, 11.b, and 13.1 amid accelerating climate change and increasing urban risk.

6. Conclusions

The increasing frequency and severity of climate-related flood events present significant challenges to urban sustainability, disaster risk management, and planning processes worldwide. In this context, this study developed and applied an operational flood detection framework using multi-temporal Sentinel-1 Synthetic Aperture Radar (SAR) imagery to investigate the severe flooding that affected Valencia, Spain, in October 2024. By integrating pre-event and post-event SAR acquisitions with systematic preprocessing and change-detection techniques, the study successfully identified and delineated flood-affected areas under adverse meteorological conditions. The analysis revealed an inundated area of approximately 4.96 km^2, with the most pronounced impacts in the western and northwestern sectors of the metropolitan region.

The findings demonstrate the considerable value of Sentinel-1 SAR observations for operational flood monitoring in urban environments. Unlike optical remote sensing systems, SAR imagery enables continuous observation regardless of cloud cover, atmospheric conditions, or daylight, making it particularly suitable for disaster situations characterized by rapidly changing environmental conditions. The successful extraction of flood extent during an extreme weather event demonstrates the ability of multi-temporal radar analysis to provide timely, reliable, and spatially explicit information that supports emergency response activities and post-disaster assessment processes.

Beyond its methodological contribution, the primary contribution of this study lies in the development of a planning-oriented conceptual framework that connects satellite-derived flood information with urban planning, disaster risk reduction, and climate adaptation processes. While many previous studies have focused primarily on improving flood detection accuracy, relatively little attention has been given to understanding how remotely sensed hazard information can be translated into planning-relevant knowledge and integrated into planning and governance processes. By explicitly linking satellite-derived flood information with the objectives of SDG Targets 11.5, 11.b, and 13.1, the study demonstrates how operational geospatial information can contribute to evidence-based planning and policy-oriented decision-making.

The proposed framework represents a step toward bridging the gap between technical flood mapping and urban planning practice. Rather than viewing flood maps solely as hazard products, the framework illustrates how Earth observation data can be transformed into planning-relevant spatial intelligence capable of supporting risk-sensitive land-use planning, flood-resilient infrastructure planning, disaster preparedness, and climate adaptation policies. In this context, satellite-derived flood information should be regarded not only as a technical monitoring product but also as a strategic planning resource that supports sustainable and adaptive urban governance.

The results further reinforce the broader understanding that urban flood risk emerges from the interaction of climatic extremes, land-use dynamics, infrastructure characteristics, and socio-spatial conditions. The Valencia case study demonstrates that extreme precipitation events become disasters not only because of meteorological intensity but also because of the spatial configuration of urban systems and their capacity to respond to disturbances. Effective flood risk reduction, therefore, requires integrated approaches that combine hazard monitoring, climate adaptation, land-use planning, infrastructure planning, and institutional preparedness within an integrated urban planning and disaster risk reduction framework.

From a sustainability perspective, the study highlights the increasing importance of geospatial information in achieving international development objectives. The United Nations 2030 Agenda emphasizes the need for evidence-based approaches to disaster risk reduction and climate adaptation, particularly in rapidly urbanizing and hazard-prone regions. The operational workflow and conceptual framework presented in this research provide a scalable and transferable approach for supporting these objectives through the generation of reliable flood information and planning-relevant spatial knowledge.

Several limitations should be acknowledged. The analysis primarily focused on flood extent and did not include information on flood depth, duration, hydrodynamic behavior, or direct socioeconomic impacts. Additionally, challenges related to SAR interpretation in dense urban environments—including radar shadowing, layover effects, and double-bounce scattering—remain important sources of uncertainty. Furthermore, the proposed framework remains conceptual and was demonstrated through a single case study.

Looking beyond Valencia, the transferability of this framework depends on the availability of comparable Sentinel-1 coverage, land-cover products, and municipal governance structures capable of absorbing satellite-derived evidence into planning practice. Cities with similarly dense urban-fluvial interfaces—for example, in the wider Mediterranean basin, where seasonal DANA-type events are common, or in other flood-prone deltaic and coastal metropolitan regions—represent natural candidates for testing the three-stage translation procedure developed here. Applying the framework across such contexts would clarify which elements (the SAR processing chain, the land-cover intersection step, or the SDG-indicator linkage) require local recalibration versus which can be adopted directly, thereby moving the framework from a single-case illustration toward a validated, cross-city planning tool.

Ultimately, the contribution of this study lies not only in mapping flood extent but in demonstrating how satellite-derived flood information can be translated into planning-relevant knowledge that supports urban planning, climate adaptation, disaster risk reduction, and sustainable urban governance. By connecting Earth observation science with planning-oriented policy frameworks, the study contributes to the growing role of geospatial information in evidence-based urban decision-making and highlights the potential of Sentinel-1 SAR observations to support more informed, adaptive, and sustainable responses to increasing flood risk under climate change across diverse urban settings.

Funding

This work received no external funding.

Institutional Review Board Statement

Not applicable.

Informed Consent Statement

Not applicable.

Data Availability Statement

The data are available on request from the corresponding author.

Conflicts of Interest

The author declares no conflict of interest.

AI Use Statement

During the preparation of this manuscript, ChatGPT (OpenAI) was used to assist with language editing and improvement of the manuscript's clarity and readability. The author subsequently reviewed and edited the content as necessary and takes full responsibility for the final content of the published article.

References

[1] Al-Wardy, M., Zarei, E., Nikoo, M.R., et al., 2026. Toward enhanced coastal flooding forecasting using deterministic and probabilistic models. Natural Hazards. 122(10), 453. DOI: https://doi.org/10.1007/s11069-026-08201-x

[2] Amitrano, D., Di Martino, G., Di Simone, A., et al., 2024. Flood detection with SAR: A review of techniques and datasets. Remote Sensing. 16(4), 656. DOI: https://doi.org/10.3390/rs16040656

[3] Zhao, J., Li, M., Li, Y., et al., 2024. Urban flood mapping using satellite synthetic aperture radar data: A review of characteristics, approaches, and datasets. arXiv preprint. arXiv:2411.04153. DOI: https://doi.org/10.48550/arXiv.2411.04153

[4] United Nations Office for Disaster Risk Reduction (UNDRR), 2015. Sendai Framework for Disaster Risk Reduction 2015–2030. UNDRR: Geneva, Switzerland. Available from: https://www.undrr.org/media/16176/download?startDownload=20260819

[5] Esmaiel, A., Abdrabo, K.I., Saber, M., et al., 2022. Integration of flood risk assessment and spatial planning for disaster management in Egypt. Progress in Disaster Science. 15, 100245. DOI: https://doi.org/10.1016/j.pdisas.2022.100245

[6] Intergovernmental Panel on Climate Change (IPCC), 2023. Climate Change 2022—Impacts, Adaptation and Vulnerability: Working Group II Contribution to the Sixth Assessment Report of the Intergovernmental Panel on Climate Change. Cambridge University Press: Cambridge, UK. DOI: https://doi.org/10.1017/9781009325844

[7] Chini, M., Pelich, R., Pulvirenti, L., et al., 2019. Sentinel-1 InSAR coherence to detect floodwater in urban areas: Houston and Hurricane Harvey as a test case. Remote Sensing. 11(2), 107. DOI: https://doi.org/10.3390/rs11020107

[8] Konapala, G., Kumar, S.V., Ahmad, S.K., 2021. Exploring Sentinel-1 and Sentinel-2 diversity for flood inundation mapping using deep learning. ISPRS Journal of Photogrammetry and Remote Sensing. 180, 163–173. DOI: https://doi.org/10.1016/j.isprsjprs.2021.08.016

[9] Otsu, N., 1979. A threshold selection method from gray-level histograms. IEEE Transactions on Systems, Man, and Cybernetics. 9(1), 62–66. DOI: https://doi.org/10.1109/TSMC.1979.4310076

[10] Tong, P., 2021. Characteristics, dimensions and methods of current assessment for urban resilience to climate-related disasters: A systematic review of the literature. International Journal of Disaster Risk Reduction. 60, 102276. DOI: https://doi.org/10.1016/j.ijdrr.2021.102276

[11] Salamatnia, A., Jozi, S.A., Malmasi, S., et al., 2019. Assessment of the temporal and spatial variations of urban development using RS and GIS: A case study—Yasuj, Iran. Journal of the Indian Society of Remote Sensing. 47(7), 1163–1172. DOI: https://doi.org/10.1007/s12524-019-00973-z

[12] Salamatnia, A., Jozi, S.A., 2021. Presenting a conceptual model for urban ecological resilience with a multi-scale approach (case study: Yasuj, Iran). Arabian Journal of Geosciences. 14(2), 104. DOI: https://doi.org/10.1007/s12517-020-06355-x

[13] United Nations Statistics Division, United Nations Office for Disaster Risk Reduction (UNDRR), 2024. SDG Indicator Metadata. UNDRR: Geneva, Switzerland. Available from: https://unstats.un.org/sdgs/metadata/files/Metadata-11-05-01.pdf

[14] Sohn, W., Kim, J.-H., Li, M.-H., et al., 2020. How does increasing impervious surfaces affect urban flooding in response to climate variability? Ecological Indicators. 118, 106774. DOI: https://doi.org/10.1016/j.ecolind.2020.106774

[15] European Space Agency, 2024. Devastating floods in Spain witnessed by satellites. Available from: https://www.esa.int/Applications/Observing_the_Earth/Devastating_floods_in_Spain_witnessed_by_satellites (cited 10 February 2026).

[16] García, P.L.M., 2025. Fact-check: AEMET's reference to Cuenca did not imply that the storm was easing over Valencia despite Mazón's claim. Available from: https://www.newtral.es/serrania-cuenca-dana-factcheck/20251104/ (cited 10 February 2026). (in Spanish)

[17] Rokkam, K.K., Rani, S., Kumar, K., et al., 2024. SAR-FM: SAR-based flood rapid mapping using multimodal data fusion. In Proceedings of the Remote Sensing for Agriculture, Ecosystems, and Hydrology XXVI, Edinburgh, UK, 16–20 September 2024. DOI: https://doi.org/10.1117/12.3031427

[18] Garshasbi, M., Alizadeh, H., Mojaradi, B., et al., 2025. Uncertainty-aware flood inundation mapping with a Bayesian deep learning framework using SAR imagery. IEEE Journal of Selected Topics in Applied Earth Observations and Remote Sensing. 18, 26716–26726. DOI: https://doi.org/10.1109/JSTARS.2025.3610403

[19] Pangi, P., Bagja, I.L., Budiati, L., et al., 2024. The evaluation of spatial planning for flood disasters using Sentinel-1 satellite imagery (case study: Central

Java Province). IOP Conference Series: Earth and Environmental Science. 1418(1), 012050. DOI: https://doi.org/10.1088/1755-1315/1418/1/012050

[20] Tupas, M.E., Roth, F., Bauer-Marschallinger, B., et al., 2024. Assessment of time-series-derived no-flood references for SAR-based Bayesian flood mapping. GIScience & Remote Sensing. 61(1), 2427304. DOI: https://doi.org/10.1080/15481603.2024.2427304

[21] Lahsaini, M., Albano, F., Albano, R., et al., 2024. A synthetic aperture radar-based robust satellite technique for timely mapping of floods. Remote Sensing. 16(12), 2193. DOI: https://doi.org/10.3390/rs16122193

[22] Jiang, X., Zeng, Z., 2025. Empowering multi-source SAR flood mapping with unsupervised learning. Environmental Research Letters. 20(1), 014006. DOI: https://doi.org/10.1088/1748-9326/ad9491

[23] Tran, K.H., Menenti, M., Jia, L., 2022. Surface water mapping and flood monitoring in the Mekong Delta using Sentinel-1 SAR Time Series and Otsu Threshold. Remote Sensing. 14(22), 5721. DOI: https://doi.org/10.3390/rs14225721

[24] Lacava, T., Albano, R., Lahsaini, M., et al., 2024. On a multitemporal analysis of Copernicus Sentinel data for a robust and near-real-time mapping of floods. In Proceedings of the 18th Plinius Conference on Mediterranean Risks, Chania, Greece, 30 September–3 October 2024. DOI: https://doi.org/10.5194/egusphere-plinius18-75

[25] Twele, A., Cao, W., Plank, S., et al., 2016. Sentinel-1-based flood mapping: A fully automated processing chain. International Journal of Remote Sensing. 37(13), 2990–3004. DOI: https://doi.org/10.1080/01431161.2016.1192304

[26] Copernicus Emergency Management Service, 2024. EMSR773: Flood in Valencia, Spain. Available from: https://mapping.emergency.copernicus.eu/activations/EMSR773/ (cited 10 February 2026).

[27] Tarpanelli, A., Mondini, A.C., Camici, S., 2022. Effectiveness of Sentinel-1 and Sentinel-2 for flood detection assessment in Europe. Natural Hazards and Earth System Sciences. 22(7), 2473–2489. DOI: https://doi.org/10.5194/nhess-22-2473-2022

[28] Palomba, G., Farasin, A., Rossi, C., 2020. Sentinel-1 flood delineation with supervised machine learning. In Proceedings of the 17th International Conference on Information Systems for Crisis Response and Management, Blacksburg, VA, USA, 24–27 May 2020; pp. 1072–1083. Available from: https://idl.iscram.org/files/giuliopalomba/2020/2298_GiulioPalomba_etal2020.pdf